Eur. Phys. J. Plus (2015) **130**: 229
DOI 10.1140/epjp/i2015-15229-7

THE EUROPEAN PHYSICAL JOURNAL PLUS

Regular Article

Influence of topology on the scale setting

G. Bergner[1,a], I. Montvay[2,b], P. Giudice[3,c], G. Münster[3,d], and S. Piemonte[3,e]

[1] Universität Bern, Institut für Theoretische Physik Sidlerstr. 5, CH-3012 Bern, Switzerland
[2] Deutsches Elektronen-Synchrotron DESY, Notkestr. 85, D-22603 Hamburg, Germany
[3] Universität Münster, Institut für Theoretische Physik, Wilhelm-Klemm-Str. 9, D-48149 Münster, Germany

Received: 9 February 2015 / Revised: 6 October 2015
Published online: 19 November 2015 –

Abstract. Recently a new method to set the scale in lattice gauge theories, based on the gradient flow generated by the Wilson action, has been proposed, and the systematic errors of the new scales t_0 and w_0 have been investigated by various groups. The Wilson flow provides also an interesting alternative smoothing procedure particularly useful for the measurement of the topological charge as a pure gluonic observable. We show the viability of this method for $\mathcal{N} = 1$ supersymmetric Yang-Mills theory by analysing the configurations produced by the DESY-Muenster Collaboration. The relation between the scale and the topological charge has been investigated showing a strong correlation. We have found that the scale has a linear dependence on the topological charge, the slope of which increases decreasing the volume and the gluino mass. Moreover we have investigated this dependence as a function of the reference parameter used to define the scale: the tuning of this parameter turns out to be fundamental for a more reliable scale setting. Similar conclusions hold for the Sommer parameter r_0.

1 Introduction

Lattice regularisation allows non-pertubative investigations of quantum field theories. The continuum space-time is discretised to a hypercubic finite lattice with spacing a. The integral over all possible configurations then has a mathematically well-defined meaning, and Monte Carlo methods can be applied to approximate expectation values of observables. The lattice spacing a is an important dimensionful parameter in the regularised theory; knowledge of its value is crucial to extrapolate physical quantities to the continuum limit $a \to 0$, to test the agreement with experimental data or simply to compare results obtained with different lattice actions. The value of the lattice spacing is implicitly defined once a dimensionful observable, for instance the mass of a particle in physical units, is chosen as input parameter to set the scale and to match simulations done with different bare parameters.

It is important to determine the scale as precisely as possible since an error on it contributes a significant part to both statistical and systematic errors of the lattice results, that propagates to the final physical predictions of Monte Carlo simulations. Therefore, the observable used to set the scale has to be chosen with special care. Various examples for this purpose have been investigated during the last two decades. In particular, three of them have been successfully tested for many different theories: the Sommer parameter r_0 and the Wilson flow scales t_0 and w_0.

The Sommer parameter r_0 was first proposed in ref. [1] as the distance r where the strong force between a static quark-antiquark pair multiplied by the squared distance, $r^2F(r)$, reaches some specified value, typically 1.0 or 1.65. The Sommer parameter is a pure gluonic observable in the sense that it requires only the computation of expectation values of Wilson loops. While this measurement is computationally inexpensive, noisy signals affect the result for the interquark force at large distances where however lattice artefacts are small. Systematic errors arise when different choices of smoothing procedures are used to improve the signal of $F(r)$ and when the fitting procedure is employed to extract the value of the parameters, increasing the complexity of the measurement of the Sommer parameter r_0.

[a] e-mail: bergner@itp.unibe.ch
[b] e-mail: montvay@mail.desy.de
[c] e-mail: p.giudice@uni-muenster.de
[d] e-mail: munsteg@uni-muenster.de
[e] e-mail: spiemonte@uni-muenster.de

Recently a new method to set the scale through the t_0 parameter has been proposed in ref. [2], based on the gradient flow generated by the Wilson gauge field action with or without Symanzik improvement [3]. A closely related method based on the parameter w_0 has been developed in ref. [4]. In this paper we compute the scale parameters t_0 and w_0 for the $\mathcal{N} = 1$ SU(2) supersymmetric Yang-Mills (SYM) theory and discuss their systematic errors. Our calculations employ the configurations generated by the DESY-Münster Collaboration [5–7]. We show that, for large flow times, correlations appear between the topological charge and scale setting quantities. As a consequence, unexpected finite volume effects do arise in the computation of w_0 and t_0. We further show that by a suitable choice of the numerical parameters that enter the determination of the scales t_0 and w_0 this effect can be reduced significantly. Similar analyses of the influence of topology on the scale setting have been presented in refs. [8,9] for the Sommer parameter r_0 and in ref. [10] in the context of the gradient flow running coupling. Our findings are relevant for simulations of Yang-Mills theories at fixed topology as have been studied for example in [11,12].

2 The Wilson flow

The Wilson flow can be considered as a continuous generalisation of stout smearing [13]. The starting point is to introduce an additional fictitious time t as fifth dimension, in the course of which the gauge fields $U_\mu(x)$ generated by Monte Carlo simulations are "continuously smoothed". The continuous smoothing procedure is specified by the partial differential equation

$$\frac{\partial}{\partial t} V_\mu(x,t) = -g^2 \left\{ \frac{\partial S_{\text{gauge}}(V_\mu(x,\tau))}{\partial V_\mu(x,\tau)} \right\} V_\mu(x,t), \tag{1}$$

similar to a diffusion equation, with boundary conditions

$$V_\mu(x,t)\big|_{t=0} = U_\mu(x). \tag{2}$$

Here $V_\mu(x,t)$ denotes the link variables at fictitious time t and $U_\mu(x)$ the original link variables.

The Wilson flow removes ultraviolet divergences and therefore local gauge invariant operators defined at positive flow time are automatically renormalised. Quantities constructed from the link variables $V_\mu(x,\tau)$ have a well-defined continuum limit and can be used to set the scale in lattice simulations.

The scale t_0 has been introduced in ref. [2] as the flow time t fulfilling

$$t^2\langle E(t)\rangle = 0.3. \tag{3}$$

Here the gauge energy $E(t)$ is defined as

$$E = \frac{1}{4} G^a_{\mu\nu} G^a_{\mu\nu}, \tag{4}$$

where $G_{\mu\nu}$ is a lattice version of the field strength tensor $F_{\mu\nu}$ which, as usual, is specified by the antisymmetric clover plaquette. The scale t_0 has the same dimension of the inverse string tension, *i.e.* length squared.

The closely related scale w_0 has been introduced in ref. [4] as the square root of the flow time t, where the condition

$$t\frac{\mathrm{d}}{\mathrm{d}t} t^2\langle E(t)\rangle = 0.3 \tag{5}$$

holds. w_0 has the dimension of a length, *i.e.* the same dimension of the lattice spacing. It has been demonstrated that w_0 is less sensitive to lattice artefacts than $\sqrt{t_0}$. According to ref. [4], the difference between the application of the Symanzik and the Wilson gauge field action in the integration of the flow equation on the lattice is not relevant. In this work we apply the Wilson action since it requires a smaller computational effort. The Wilson flow has been numerically integrated using a Runge-Kutta scheme with steps of length 0.01, as described in appendix C of ref. [2].

3 Measuring the scale setting quantities r_0, w_0 and t_0

The gauge configurations have been generated by the *Two-Step Polynomial Hybrid Monte Carlo* (TSPHMC) update algorithm [14,15] for the study of the hadron spectrum in SYM with gauge group SU(2) [5–7]. This theory describes the interactions between gluons and their supersymmetric partners, the gluinos. The gluino is a Majorana fermion in the adjoint representation of the gauge group. The Symanzik improved action has been used for the gauge action, and the Wilson-Dirac operator with one-level stout smeared links for the fermion action[1]. We have determined the Wilson flow scales for three different values of $\beta = 4/g^2$, where g is the bare gauge coupling, and many different values of the fermionic hopping parameter $\kappa = 1/(2m+8)$, where m is the bare gluino mass.

[1] The value of the stout smearing parameter was $\rho = 0.15$, see [6] for further details.

Table 1. Results for the adjoint pion mass m_π, the scales t_0, w_0 and the autocorrelation time $\tau(t_0)$ of t_0.

Volume	β	κ	am_π	$\sqrt{t_0}/a$	w_0/a	$\tau(t_0)$
$24^3 \times 48$	1.60	0.15500	0.5788(16)	1.5672(13)	1.5102(14)	21
$24^3 \times 48$	1.60	0.15700	0.3264(23)	1.7904(11)	1.7292(37)	10
$24^3 \times 48$	1.60	0.15750	0.2015(93)	1.8986(53)	1.8410(63)	42
$32^3 \times 64$	1.75	0.14900	0.2385(4)	3.1438(67)	2.9838(59)	50
$32^3 \times 64$	1.75	0.14920	0.2035(5)	3.270(17)	3.097(25)	45
$32^3 \times 64$	1.75	0.14940	0.1604(15)	3.362(15)	3.205(20)	35
$32^3 \times 64$	1.75	0.14950	0.1294(24)	3.551(36)	3.413(40)	65
$32^3 \times 64$	1.90	0.14387	0.2123(4)	5.73(13)	5.57(19)	440
$32^3 \times 64$	1.90	0.14415	0.1742(4)	5.71(12)	5.49(11)	296
$32^3 \times 64$	1.90	0.14435	0.1413(6)	5.96(12)	5.76(14)	502

The integration of the Wilson flow equation has been performed on every sixth thermalised configurations[2], and the results are summarised in table 1. The scales w_0 and $\sqrt{t_0}$ show only a small dependence on the gluino mass for a given β. Employing a mass-independent renormalisation scheme, the scales are extrapolated to the chiral limit at zero renormalised gluino mass and the obtained value is used to set the scale at all gluino masses. The tuning of the gluino mass is necessary for restoration of supersymmetry in the continuum limit [16,17]. In our calculations the renormalised gluino mass is represented by the square of the (adjoint) pion mass (m_π), which is defined in a partially quenched theory and can be measured with a reasonable precision. As shown in [18], the gluino mass is proportional to the square of m_π.

The Sommer parameter r_0 has been measured by first extracting the static potential $V(r)$ from the Wilson loops $W(r,t)$

$$V(r) = \lim_{t\to\infty} \ln\left(\frac{W(r,t)}{W(r,t+1)}\right) \tag{6}$$

by a suitable fit and then fitting the result to the function

$$V(r) = \sigma r - \frac{c_1}{r} + c_2. \tag{7}$$

Four levels of APE smearing with $\alpha = 0.5$ have been applied to reduce the noise of the expectation value of Wilson loops $W(r,t)$ for large r and t.

3.1 Matching the β-function

The Callan-Symanzik β-function has been determined for the $\mathcal{N} = 1$ SYM theory in ref. [19] by instanton calculations with the result

$$\beta(g) = \mu\frac{\mathrm{d}}{\mathrm{d}\mu}g(\mu) = -\frac{g^3}{16\pi^2}\frac{3N_c}{1-\frac{N_c g^2}{8\pi^2}}\,. \tag{8}$$

Within the scheme used there the β-function is exact due to the non-renormalisation theorem [19], see also [20] for an explicit proof. The first two perturbative coefficients are scheme independent, as it is well known. For the comparison with our numerical data, see below, the scheme-dependence of the higher terms actually does not have a significant effect and we thus use the expression above. The β-function can be used to compare lattice results at different bare gauge couplings g. If finite volume corrections and lattice discretisation errors can be neglected, the Wilson flow parameters t_0 and w_0 are expected to scale according to

$$\frac{w_0(g_1)}{w_0(g_2)} = \exp\left(F(g_1) - F(g_2)\right), \tag{9}$$

where the function $F(g)$ is the integral of the inverse of the β-function,

$$F(g) = \int^g \frac{\mathrm{d}g'}{\beta(g')} = \frac{8\pi^2}{3N_c g^2} + \frac{2}{3}\ln g, \tag{10}$$

up to an unessential integration constant.

[2] The individual configurations are separated by 1 unit in HMC time, $T_{\mathrm{MC}} = 1$, the measured configurations are separated by 6 units in HMC time, skipping the first 500 configurations. The integrated autocorrelation time of the unsmeared plaquette is always below 1.5 in these units.

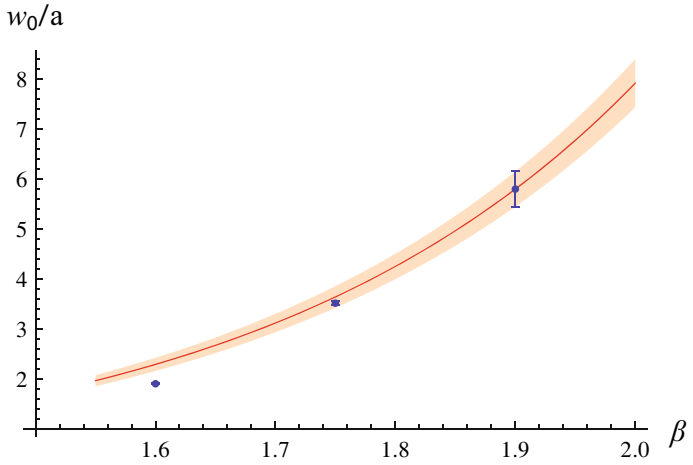

Fig. 1. Scaling of w_0 compared to the expected behaviour from the β-function (red line). The orange band represents the statistical error determined by eq. (9).

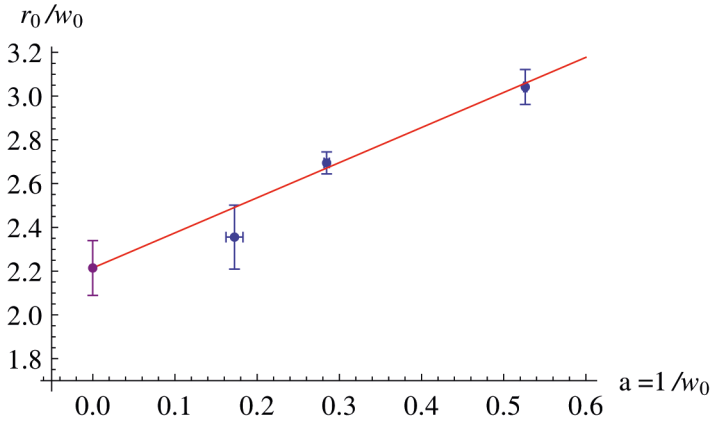

Fig. 2. Extrapolation of the dimensionless ratio r_0/w_0 to the continuum limit.

For our case, $N_c = 2$, the scaling according to eq. (9) has been checked by taking the value of w_0 at $\beta = 4/g^2 = 1.9$ as reference point, see fig. 1. The agreement with eq. (9) is rather good.

The relative deviation from the scaling,

$$K = \frac{w_0(1.9)}{w_0(\beta)} \left(\frac{1.9}{\beta}\right)^{1/3} \exp\left\{\frac{\pi^2(\beta - 1.9)}{3}\right\}, \tag{11}$$

is $K = 1.03(6)$ for $\beta = 1.75$ and $K = 1.20(8)$ for $\beta = 1.6$. The larger deviation at $\beta = 1.6$ is presumably due to lattice artefacts and/or higher order terms in the lattice β-function.

3.2 Extrapolation of the ratio r_0/w_0 to the continuum limit

The ratio of the Sommer parameter r_0 to the Wilson flow scale w_0 computed on the lattice is expected to scale in the continuum limit as

$$\lim_{a\to 0} \frac{r_0(a)}{w_0(a)} = \frac{r_0}{w_0}(1 + O(a)), \tag{12}$$

due to the lattice artefacts coming from the Wilson discretisation of the fermion part of the action. The linear fit of our data is presented in fig. 2, where the lattice spacing a has been defined implicitly in terms of $1/w_0$. The final result extrapolated to the continuum limit is

$$\lim_{a\to 0} \frac{r_0(a)}{w_0(a)} = 2.21(12), \tag{13}$$

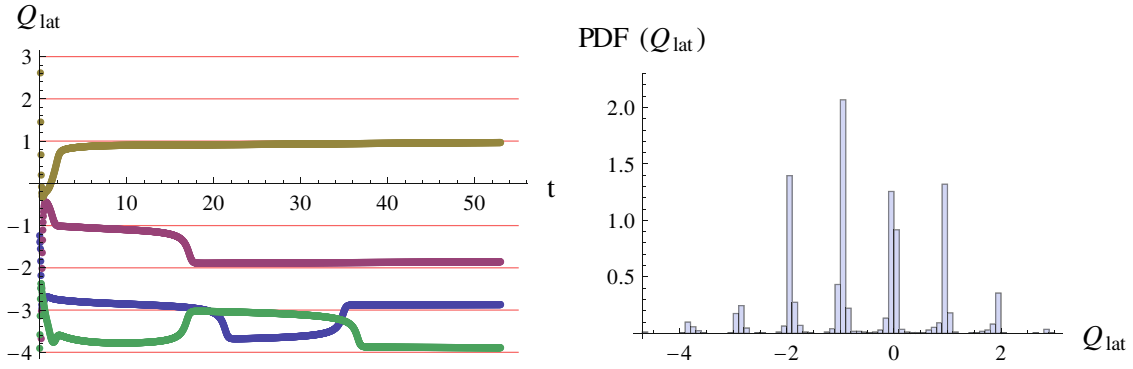

(a) $Q_{\rm lat}\,(t)$ (b) PDF ($Q_{\rm lat}$)

Fig. 3. (a) Topological charge for four different configuration as a function of the flow time t on a $32^3 \times 64$ lattice, $\beta = 1.9$ and $\kappa = 0.14435$. (b) Distribution of the topological charge at $t = 50$ for the same run.

and it allows to express w_0 in physical units

$$w_0 \simeq 0.226(12)\,\text{fm}, \tag{14}$$

assuming length scales to be set by QCD units, where the value of r_0 is given by $r_0 \simeq 0.5\,\text{fm}$. In these units the spatial extent of the lattice used for the simulations at $\beta = 1.9$ is therefore

$$L \simeq 1.27\,\text{fm}, \tag{15}$$

which is large enough to avoid finite volume corrections to masses of the bound spectrum of the theory, as has been shown in [5]. The corresponding lattice spacing is

$$a(\beta = 1.9) \simeq 0.04\,\text{fm}. \tag{16}$$

4 Measuring the topological charge with the Wilson flow

The topological charge is defined for a given field configuration in the continuum by the integral

$$Q_{\rm top} = \frac{1}{32\pi^2} \int \mathrm{d}^4x\, \epsilon_{\mu\nu\rho\sigma} F_a^{\mu\nu} F_a^{\rho\sigma}. \tag{17}$$

On the lattice we define the topological charge with the same antisymmetric discretisation of the field strength tensor as used for the flow equation:

$$Q_{\rm lat} = \frac{1}{32\pi^2} \sum_x \epsilon_{\mu\nu\rho\sigma} G_a^{\mu\nu} G_a^{\rho\sigma}. \tag{18}$$

This *lattice topological charge* is affected by ultraviolet fluctuations, and its value is in general not an integer. A possible solution to this problem is a smoothing procedure to suppress the short distance fluctuations and to recover a well-defined topological charge in the continuum limit [21]. We have applied the Wilson flow as smoothing procedure, comparing the results with APE and stout smearing, as done in ref. [22].

As shown in fig. 3(a), for large enough flow time t the topological charge reaches a near integer value and the topological susceptibility shows a plateau. Actually, after a very long number of iterations, in our case of the order 400 at $\beta = 1.9$, when the smoothing starts to affect long range fluctuations, the topological charge drops to zero. This does, however, not impair the presence of a clear plateau.

Following ref. [22], we convert the raw lattice topological charge to an integer using

$$Q_{\rm top} = \text{round}(\alpha Q_{\rm lat}(t)), \tag{19}$$

where the flow time t is chosen for definiteness to be

$$t = w_0(\beta)^2, \tag{20}$$

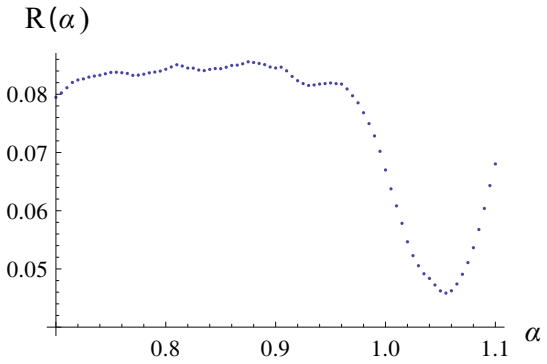

Fig. 4. Plot of $R(\alpha)$ for the lattice $32^3 \times 64$ at $\beta = 1.75$ and $\kappa = 0.1494$. The minimum of $R(\alpha)$ is located at $\alpha = 1.055$.

Table 2. Results for the topological susceptibility obtained using the Wilson Flow (WF) and 250 levels of APE smearing with $\alpha = 0.1$.

Run	Volume	β	κ	$(a^4\chi_{\rm top}) \times 10^{-6}$ (WF)	$(a^4\chi_{\rm top}) \times 10^{-6}$ (APE)
A1	$24^3 \times 48$	1.60	0.15500	131(14)	132(21)
A2	$24^3 \times 48$	1.60	0.15700	100(8)	78(14)
A3	$24^3 \times 48$	1.60	0.15750	81(5)	70(9)
B1	$32^3 \times 64$	1.75	0.14900	15(2)	16(2)
B2	$32^3 \times 64$	1.75	0.14920	11(1)	12(1)
B3	$32^3 \times 64$	1.75	0.14940	10(1)	10(1)
B4	$32^3 \times 64$	1.75	0.14950	7(1)	9(2)
C1	$32^3 \times 64$	1.90	0.14387	0.82(15)	0.90(18)
C2	$32^3 \times 64$	1.90	0.14415	1.39(20)	1.53(29)
C3	$32^3 \times 64$	1.90	0.14435	0.81(10)	0.98(16)

and where the scale $w_0(\beta)$ is defined in the chiral limit and therefore depends only on the gauge coupling. This value of t is chosen sufficiently large to remove the cut-off effects; but not too large to change the number of instantons and the final value of the topological charge [23]. The real constant α is chosen to minimise the expectation value [24]

$$R(\alpha) = \langle (\alpha Q_{\rm lat} - \mathrm{round}(\alpha Q_{\rm lat}))^2 \rangle. \tag{21}$$

Near the continuum limit it is expected that $\alpha \approx 1$, *i.e.* the distribution of $Q_{\rm lat}$ is already centred near integer values without requiring an additional multiplicative renormalisation, see figs. 3(b) and fig. 4. In addition, the topological susceptibility $\chi_{\rm top}$, defined by

$$\chi_{\rm top} = \frac{\langle Q_{\rm top}^2 \rangle - \langle Q_{\rm top} \rangle^2}{V} = \frac{\langle Q_{\rm top}^2 \rangle - \langle Q_{\rm top} \rangle^2}{a^4 N_s^3 N_t}\,, \tag{22}$$

where V is the volume of the system, has been measured. The results are shown in table 2 and in fig. 5. A good agreement has been observed between the topological susceptibility obtained with the Wilson flow and with APE smearing. The value of $\chi_{\rm top}$ extrapolated to the chiral limit confirms the *topological suppression* for SYM mentioned in ref. [25]. The extrapolation to the continuum limit supports the assumption that the remaining non-zero value observed in the chiral limit at fixed β is only a lattice artefact.

5 Autocorrelation time of flow observables

The autocorrelation time of the topological charge increases drastically near the continuum limit and may even result in *topological freezing*. Whether this fact occurs or not depends, however, on the chosen boundary conditions [26,27]. The scales w_0 and t_0 exhibit a very long autocorrelation time, especially near the continuum limit, similarly to the topological charge. Our configurations have been produced with the usual periodic boundary conditions and we observe the expected increase of the autocorrelations.

The autocorrelation time should scale with the lattice spacing a asymptotically as a^{-z}, where $z = 1$ for Hybrid Monte Carlo (HMC) algorithms for free field theory. In our runs the lattice spacing is decreased roughly by a factor

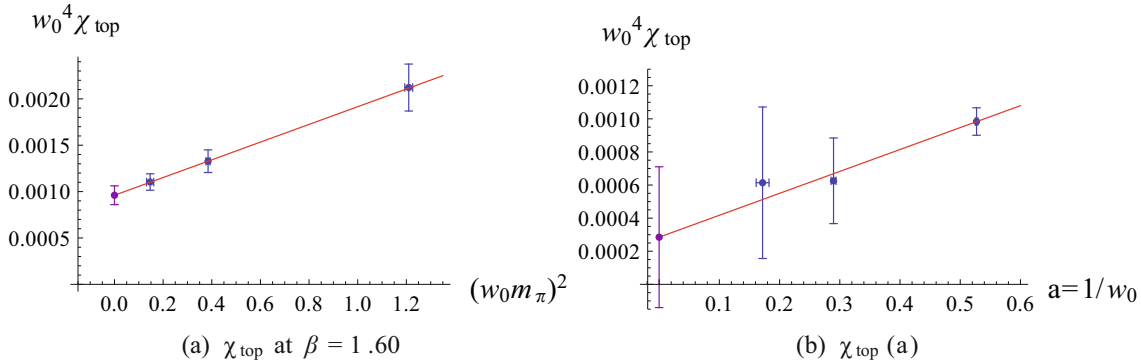

Fig. 5. Extrapolation of the topological susceptibility χ_{top} (a) to the chiral limit on a $32^3 \times 64$ lattice at $\beta = 1.60$ and (b) to the continuum limit.

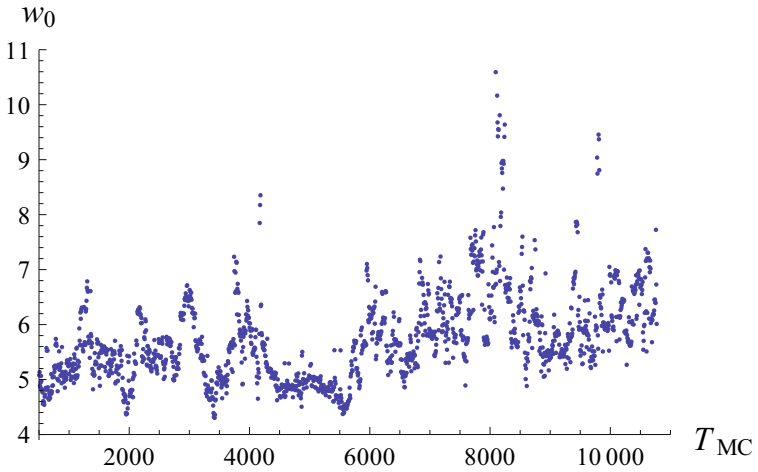

Fig. 6. Monte Carlo history of w_0 on a $32^3 \times 64$ lattice, $\beta = 1.9$ and $\kappa = 0.14435$. T_{MC} is the Monte Carlo time. w_0 is measured every sixth configurations.

2.5 between $\beta = 1.6$ and $\beta = 1.9$. The autocorrelation time $\tau(t_0)$ of t_0 at $\beta = 1.9$ is, however, approximately twelve times larger than at $\beta = 1.6$, see table 1.

Although the interval between $\beta = 1.6$ and $\beta = 1.9$ is presumably not yet in the asymptotic regime, the variation of $\tau(t_0)$ seems to indicate a value $z > 2$ and a possible connection of the topological charge with the flow observables used to set the scale.

6 Correlations between topological charge and the scale w_0

In order to investigate the nature of the long autocorrelation of w_0, we have considered its Monte Carlo history. The scale w_0 can be defined for a single configuration without the need of an ensemble average by determining the flow time when the integrated flow matches the condition specified by eq. (5). In fig. 6 the Monte Carlo history of w_0 is shown for a lattice $32^3 \times 64$ at $\beta = 1.9$ and $\kappa = 0.14435$. One can see that the value of w_0 has large fluctuations with a long period. In particular, very strong upward spikes emerge.

Wilson flow scales depend implicitly on the reference value chosen in eq. (5). Small reference values will potentially produce large lattice artefacts on the final results, while w_0 and t_0 will be affected by non-negligible finite volume effects for larger reference values. Let us define the scale w_0^u to be the square root of the flow time when the condition

$$t\frac{\mathrm{d}}{\mathrm{d}t}t^2\langle E(t)\rangle = u \tag{23}$$

is satisfied. By varying u, one can study how the autocorrelations are affected by different choices of the reference value. Here and in the following we set $w_0 \equiv w_0^{0.3}$. In fig. 7 the Monte Carlo histories of $w_0^{0.1}$, $w_0^{0.3}$ and $w_0^{0.4}$ are compared. When the value of u is small the fluctuations and spikes are significantly reduced. On the other hand, when the value

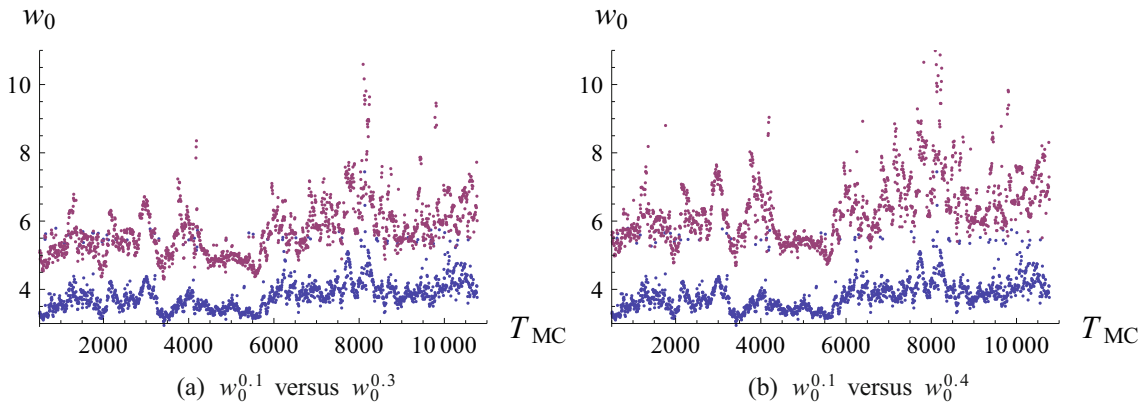

Fig. 7. Comparison of the Monte Carlo history (a) of $w_0^{0.1}$ (blue) with $w_0^{0.3}$ (red) and (b) of $w_0^{0.1}$ (blue) with $w_0^{0.4}$ (red), on a $32^3 \times 64$ lattice, $\beta = 1.9$ and $\kappa = 0.14435$. The magnitude of the peaks increases drastically when the reference value to set the w_0 scale is larger.

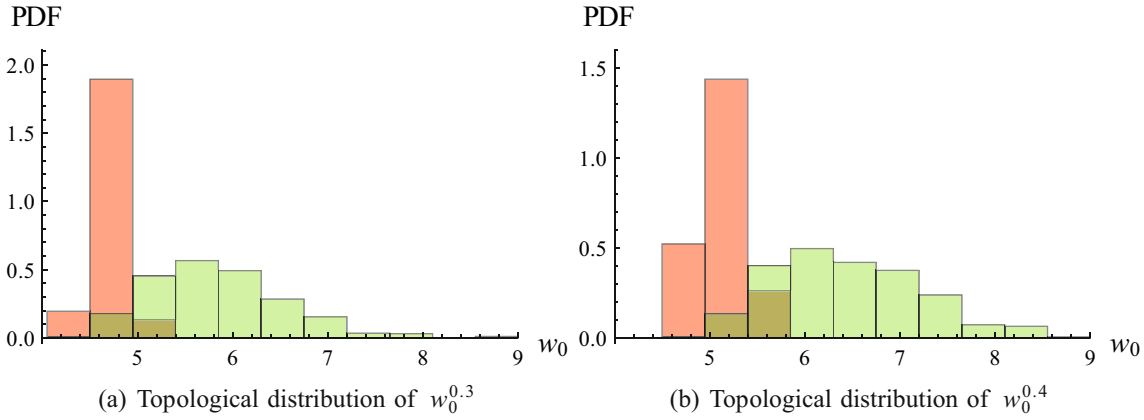

Fig. 8. Probability distribution function of (a) $w_0^{0.3}$ and of (b) $w_0^{0.4}$ restricted to the topological sector $|Q_{\text{top}}| = 1$ (green) and $|Q_{\text{top}}| = 4$ (red) on a $32^3 \times 64$ lattice, $\beta = 1.9$ and $\kappa = 0.14435$.

of u is increased the spikes become even more pronounced. Increasing the value of u leads to a larger flow time needed to match the condition (23), which means that a stronger smoothing induced by the flow equation is applied to the configurations. Large flow times will more effectively remove ultraviolet fluctuations, and the system will be brought towards a classical configuration, as observed in sect. 4. Therefore one might argue that spikes and large fluctuations are related to topological effects. Using the results presented in sect. 4 we have been able to compute the value of w_0^u restricted only to configurations with a fixed definite topological charge.

The distributions of $w_0^{0.4}$ and $w_0^{0.3}$ are shown for the same run in fig. 8 for two selected topological sectors, $|Q_{\text{top}}| = 1$ and $|Q_{\text{top}}| = 4$. The distribution of $w_0^{0.3}$ restricted to the topological sector $|Q_{\text{top}}| = 1$ is rather broad and the average value is larger than for the distribution in the topological sector $|Q_{\text{top}}| = 4$. The same behaviour appears for the restricted distributions of $w_0^{0.4}$, but with a slightly larger difference between the two mean values of the distributions. This result clearly shows that there is a correlation between the value of w_0 and the topological charge, not only in terms of its mean value but also in terms of its distribution. The largest fluctuations observed in fig. 6 are produced by the configurations at low values of the topological charge, where the distribution of w_0 is broad. The long periodicity is induced by the transitions during the Monte Carlo update time between topological sectors around zero, characterised by large expectation value of w_0, and topological sectors far from the origin with a small mean value of w_0. The Monte Carlo history restricted to a given topological sector is presented in fig. 9.

In fig. 10 we present the expectation value of w_0^u restricted to the various topological sectors for four different values of u, in the same run on a $32^3 \times 64$ lattice, with $\beta = 1.9$ and $\kappa = 0.14435$. The behaviour of $w_0^u(|Q_{\text{top}}|)$ is approximately linear for all u but it has a steeper slope when the reference scale u is larger. We have used a linear fit of the form

$$\langle w_0^u \rangle (|Q_{\text{top}}|) = s|Q_{\text{top}}| + q. \tag{24}$$

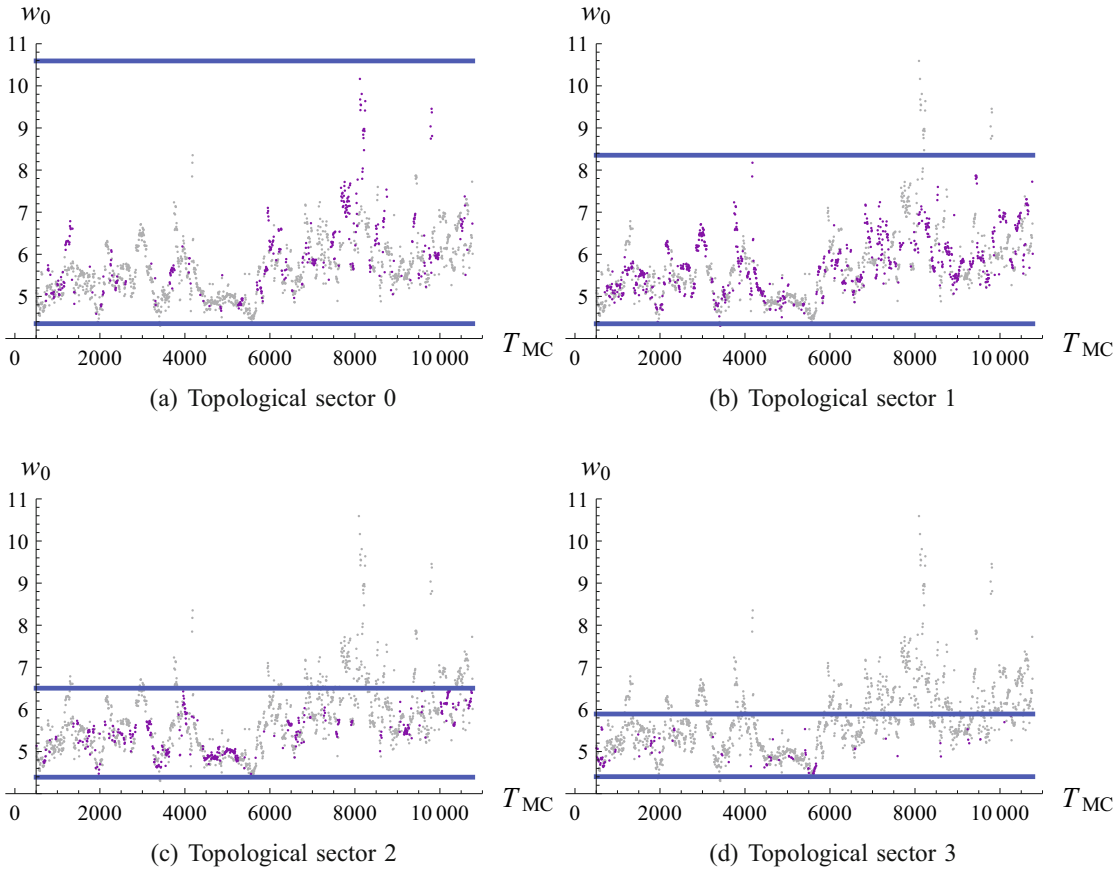

Fig. 9. Monte Carlo history of the w_0 on a $32^3 \times 64$ lattice, $\beta = 1.9$ and $\kappa = 0.14435$. The purple points highlight the value of w_0 only for configurations characterised by a given topological sector; the blue lines mark its maximal and minimal value.

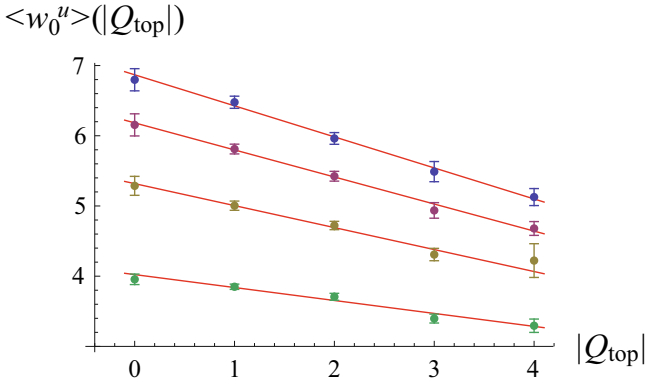

Fig. 10. Linear fit of the dependence of w_0^u on the topological charge for u equal to 0.1 (green), 0.2 (yellow), 0.3 (purple) and 0.4 (blue) for a lattice $32^3 \times 64$, $\beta = 1.9$ and $\kappa = 0.14435$.

The resulting slope coefficients s are presented as a function of u in fig. 11(a). The modulus of the slope s increases increasing u. This means that the dependence of w_0^u on the topology is stronger when u is larger. This behaviour confirms our previous claim about the topological origin of the spikes in fig. 7: when u is large the smoothing effects of the Wilson flow are large and the configuration is driven towards a classical one where the influence of the topology is stronger. As a result, the integrated autocorrelation time of $w_0^{0.4}$ is around 800 T_{MC}, approximately three times larger than the autocorrelation time of $w_0^{0.1}$, which is around 300 T_{MC}. We have also investigated the dependence of s on the adjoint pion mass squared, observing that it increases as one approaches the chiral limit, see fig. 11(b).

The dependence of the flow scale on the topological charge can be interpreted as a finite volume effect [11,12]. To address this point we repeated the same systematic analysis on the lattice $32^3 \times 64$ at $\beta = 1.75$, where the physical

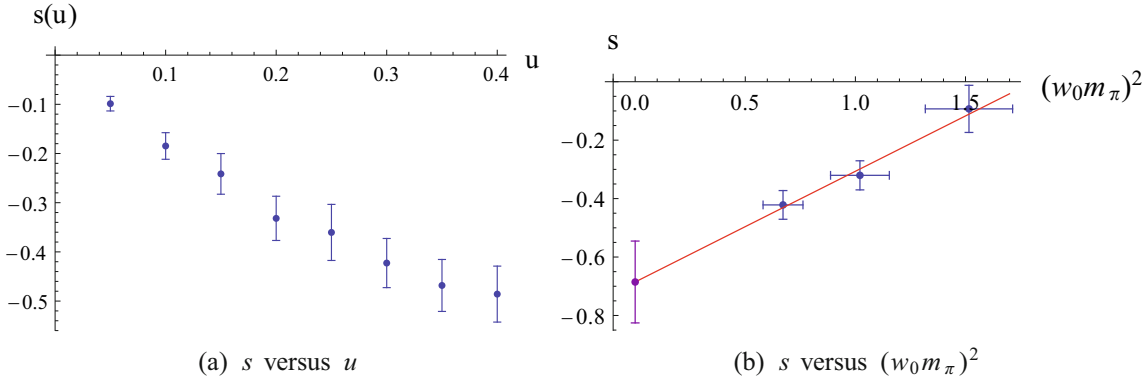

Fig. 11. (a) Slope coefficient s as a function of the reference value u for the lattice $32^3 \times 64$, $\beta = 1.9$ and $\kappa = 0.14435$. (b) Slope coefficient s as a function of $(w_0 m_\pi)^2$ at $\beta = 1.9$ for $w_0^{0.3}$. The value of s linearly extrapolated to the chiral limit is $s((w_0 m_\pi)^2 = 0) = -0.69(14)$.

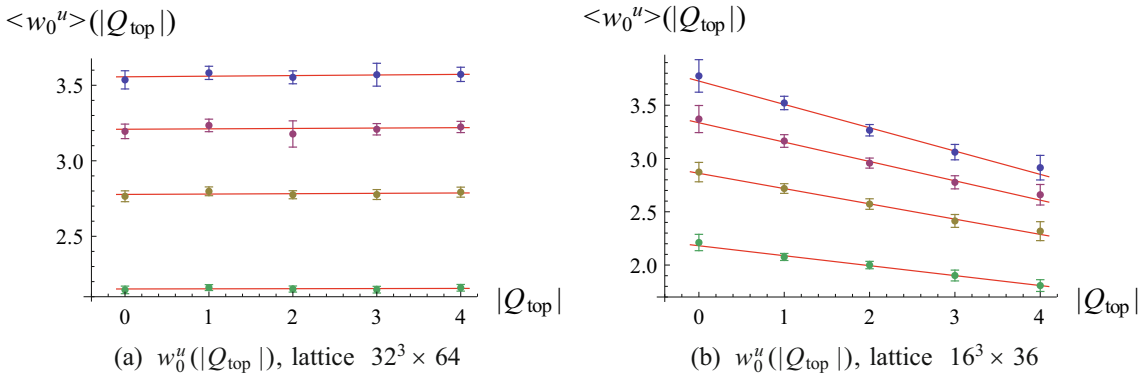

Fig. 12. The same as fig. 10, but for (a) the lattice $32^3 \times 64$, $\beta = 1.75$ and $\kappa = 0.1494$; (b) the lattice $16^3 \times 36$, $\beta = 1.75$ and $\kappa = 0.1490$.

volume is approximately seven times larger than at $\beta = 1.9$. The dependence of the various w_0^u on $|Q_{\text{top}}|$ is presented in fig. 12(a). As the figure shows, in this large physical volume the dependence of the flow scales on the topology completely disappears. If instead, the physical volume is shrunk again by simulating on a $16^3 \times 36$ lattice at the same $\beta = 1.75$, the observables w_0^u appear to depend on the topological charge $|Q_{\text{top}}|$ as before, see fig. 12(b). Note that the value of κ used in the smaller volume is smaller than the first case, but according to fig. 11(b) this should even reduce the slope. This demonstrates that finite volume effects are the origin of the dependence of w_0 on the topological charge in the runs on the finer lattices at $\beta = 1.9$.

7 Correlations between topological charge and the scale r_0

The Sommer parameter depends on the reference value c used to implicitly define r_0 through the equation

$$r_0^2 F(r_0) = c. \tag{25}$$

In QCD the value $c = 1.65$ has been chosen to optimise the signal-to-noise ratio versus lattice artifacts in $F(r)$ for small distances [1]. The role of c is similar to that of u in the definition of w_0, therefore it makes sense to ask whether also r_0 exhibits the same behaviour observed for w_0 in the section before.

To this end, the parameter r_0^c has been computed from the fit of Wilson loops measured only on configurations with a given topological charge. The dependence of $r_0^{1.65}$ on the topological sector is presented in fig. 13(a) for the lattice $32^3 \times 64$, $\beta = 1.9$ and $\kappa = 0.14415$. The function $r_0^{1.65}(|Q_{\text{top}}|)$ is linear like in the case of w_0. As before, we fit the linear behavior of $r_0^c(|Q_{\text{top}}|)$ by

$$\langle r_0^c \rangle(|Q_{\text{top}}|) = s|Q_{\text{top}}| + q, \tag{26}$$

for different values of c. The resulting slope coefficients s are presented as a function of c in fig. 13(b). The slope coefficient is larger when the reference value c increases. The influence of the topology on the scale r_0^c is therefore

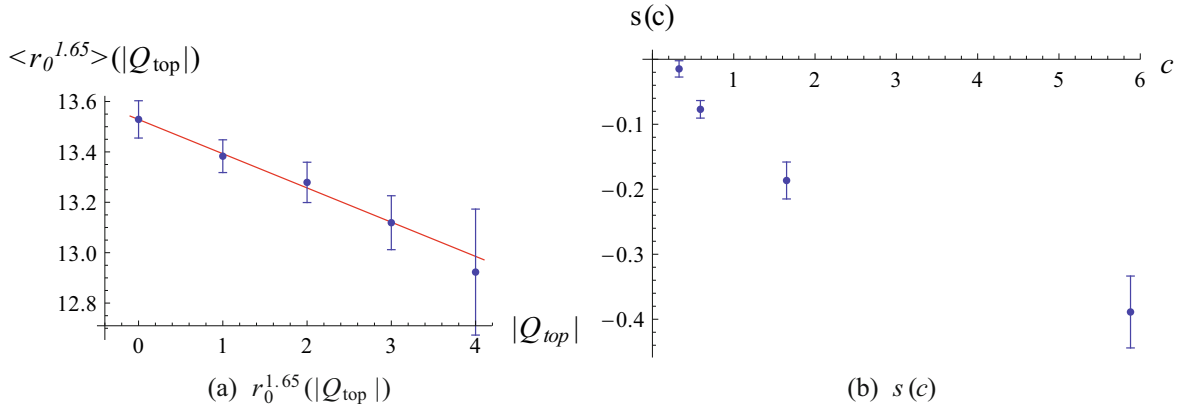

Fig. 13. Results for the Sommer parameter r_0^c on the lattice $32^3 \times 64$, $\beta = 1.9$ and $\kappa = 0.14415$. (a) Dependence of $r_0^{1.65}$ on the topological sector. (b) Slope coefficient s as a function of the reference value c.

Table 3. Results for the scale w_0^u.

Run	$w_0^{0.05}$	$w_0^{0.10}$	$w_0^{0.15}$	$w_0^{0.20}$	$w_0^{0.25}$	$w_0^{0.30}$	$w_0^{0.35}$	$w_0^{0.40}$
A1	0.6419(10)	0.9587(15)	1.1420(17)	1.2844(19)	1.4048(22)	1.5104(21)	1.6046(26)	1.6901(26)
A2	0.7767(15)	1.1136(22)	1.3192(27)	1.4787(34)	1.6122(40)	1.7290(43)	1.8319(46)	1.9268(44)
A3	0.8341(23)	1.1853(35)	1.4048(41)	1.5760(47)	1.7182(53)	1.8419(60)	1.9511(58)	2.0495(68)
B1	1.5087(42)	2.0058(51)	2.3331(56)	2.5878(60)	2.8011(62)	2.9838(59)	3.1495(62)	3.3012(62)
B2	1.5610(84)	2.082(15)	2.417(19)	2.684(19)	2.904(23)	3.097(25)	3.256(27)	3.424(25)
B3	1.6113(74)	2.151(12)	2.504(13)	2.779(17)	3.005(18)	3.205(20)	3.385(22)	3.551(25)
B4	1.6957(15)	2.269(24)	2.651(28)	2.955(34)	3.205(37)	3.413(41)	3.623(43)	3.793(42)
C1	2.734(46)	3.687(81)	4.35(10)	4.82(14)	5.24(16)	5.60(18)	5.90(18)	6.19(18)
C2	2.717(40)	3.666(85)	4.31(11)	4.76(13)	5.13(13)	5.49(13)	5.78(15)	6.05(14)
C3	2.855(44)	3.822(81)	4.47(11)	4.97(11)	5.40(14)	5.76(14)	6.08(15)	6.38(15)

similar to that of w_0^u, even though both the relative variation of r_0^c between different topological sectors and the slope coefficient s seem to be smaller in the case of r_0. For instance, on the lattice $32^3 \times 64$, $\beta = 1.9$ and $\kappa = 0.14415$, the slope coefficient s for $w_0^{0.3}$ is $s = -0.35(5)$, which is almost twice as large as $s = -0.19(3)$ of $r_0^{1.65}$.

8 Conclusions

We have presented a detailed analysis of the Wilson flow observables w_0, used to set the scale alternatively to the Sommer parameter r_0. The same analysis has been done also for t_0 and r_0, reaching similar conclusions. In finite volumes we observed a substantial dependence of w_0 on the topological charge, in agreement with the previous discussion on this topic for the Sommer parameter r_0 of refs. [8,9]. We have found, however, that r_0 seems to suffer less this dependence compared to the Wilson flow scales, when the standard references $u = 0.3$ and $c = 1.65$ are used.

Scales based on the Wilson flow require a delicate fine-tuning to correctly handle finite volume effects and errors due to lattice artefacts. A result free of *topological* finite volume effects can be obtained if there is no coupling between the scale and the topological charge, up to the statistical precision. The final result has fairly small statistical and systematic errors, therefore w_0 can be used to set the scale in extrapolations to the chiral and continuum limit. Our observations support the use of small flow times to set the scale, at least for our model and within our present precision: the ratio of w_0^u and $w_0^{0.3}$ is flat for $u \gtrsim 0.1$ (see table 3 and fig. 14).

The findings presented in this article have been obtained in the context of our investigation of SYM theory. For other theories like QCD, with a different number of colours and a different fermion content, the details may be different. However, the fact that a dependence of the scale on topology emerges for sufficient large reference scales does not rely on particular properties of SYM and will hold for other theories as well. We therefore encourage systematic studies in this direction, in particular considering that there are proposals, like in [28], to increase the value of the reference flow time.

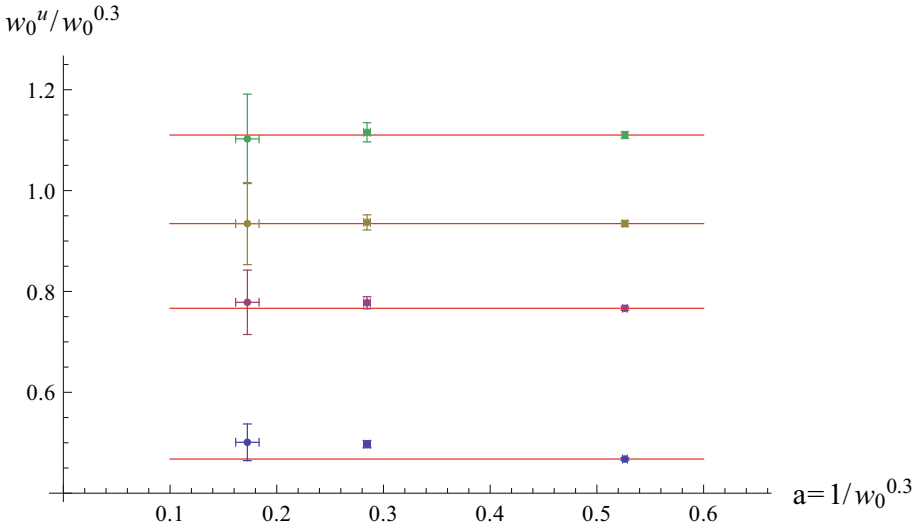

(a) $w_0^u/w_0^{0.3}$ for $u = 0.05$ (blue), $u = 0.15$ (purple), $u = 0.25$ (yellow), $u = 0.35$ (green).

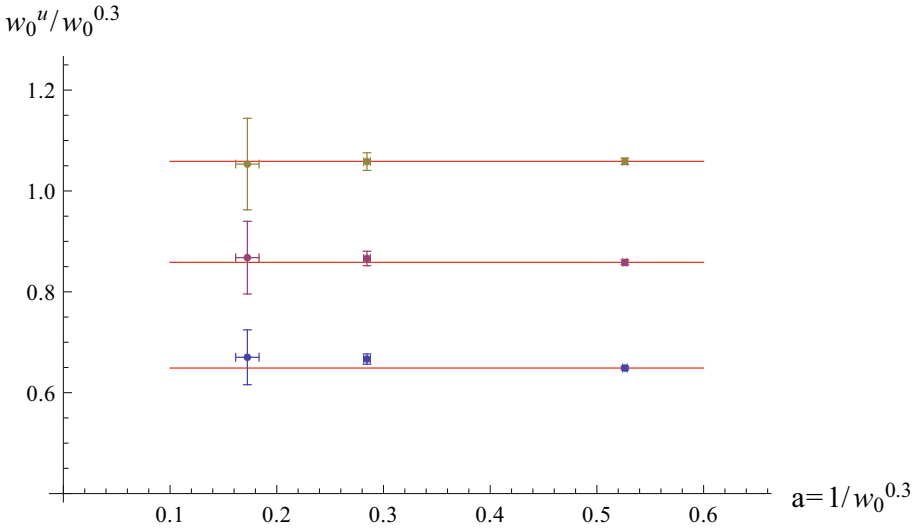

(b) $w_0^u/w_0^{0.3}$ for $u = 0.10$ (blue), $u = 0.20$ (purple), $u = 0.40$ (yellow).

Fig. 14. Scaling of the various w_0^u with respect to $w_0^{0.3}$ as a function of the lattice spacing. The scaling is flat within the errors for $u \gtrsim 0.15$.

The authors gratefully acknowledge the Gauss Centre for Supercomputing (GCS) for providing computing time for a GCS Large Scale Project on the GCS share of the supercomputer JUQUEEN at Jülich Supercomputing Centre (JSC). GCS is the alliance of the three national supercomputing centres HLRS (Universität Stuttgart), JSC (Forschungszentrum Jülich), and LRZ (Bayerische Akademie der Wissenschaften), funded by the German Federal Ministry of Education and Research (BMBF) and the German State Ministries for Research of Baden-Württemberg (MWK), Bayern (StMWFK) and Nordrhein-Westfalen (MIWF).

References

1. R. Sommer, Nucl. Phys. B **411**, 839 (1994) arXiv:hep-lat/9310022.
2. M. Lüscher, JHEP **08**, 071 (2010) arXiv:1006.4518 [hep-lat].
3. R. Narayanan, H. Neuberger, JHEP **03**, 064 (2006) arXiv:hep-th/0601210.
4. S. Borsanyi *et al.*, JHEP **09**, 010 (2012) arXiv:1203.4469 [hep-lat].
5. G. Bergner, T. Berheide, I. Montvay, G. Münster, U.D. Özugurel, D. Sandbrink, JHEP **09**, 108 (2012) arXiv:1206.2341 [hep-lat].
6. G. Bergner, I. Montvay, G. Münster, U.D. Özugurel, D. Sandbrink, JHEP **11**, 061 (2013) arXiv:1304.2168 [hep-lat].

7. K. Demmouche, F. Farchioni, A. Ferling, I. Montvay, G. Münster, E.E. Scholz, J. Wuilloud, Eur. Phys. J. C **69**, 147 (2010) arXiv:1003.2073 [hep-lat].
8. F. Bruckmann, F. Gruber, K. Jansen, M. Marinkovic, C. Urbach, M. Wagner, Eur. Phys. J. A **43**, 303 (2010) arXiv:0905.2849 [hep-lat].
9. JLQCD Collaboration (S. Aoki *et al.*), Phys. Rev. D **78**, 014508 (2008) arXiv:0803.3197 [hep-lat].
10. P. Fritzsch, A. Ramos, F. Stollenwerk, PoS **Lattice2013**, 461 (2014) arXiv:1311.7304 [hep-lat].
11. R. Brower, S. Chandrasekharan, J.W. Negele, U.J. Wiese, Phys. Lett. B **560**, 64 (2003) arXiv:hep-lat/0302005.
12. S. Aoki, H. Fukaya, S. Hashimoto, T. Onogi, Phys. Rev. D **76**, 054508 (2007) arXiv:0707.0396 [hep-lat].
13. C. Morningstar, M.J. Peardon, Phys. Rev. D **69**, 054501 (2004) arXiv:hep-lat/0311018.
14. I. Montvay, E.E. Scholz, Phys. Lett. B **623**, 73 (2005) arXiv:hep-lat/0506006.
15. E.E. Scholz, I. Montvay, PoS **LAT2006**, 037 (2006) arXiv:hep-lat/0609042.
16. G. Curci, G. Veneziano, Nucl. Phys. B **292**, 555 (1987).
17. H. Suzuki, Nucl. Phys. B **861**, 290 (2012). arXiv:1202.2598 [hep-lat].
18. G. Münster, H. Stüwe, JHEP **05**, 034 (2014) arXiv:1402.6616 [hep-th].
19. V.A. Novikov, M.A. Shifman, A.I. Vainshtein, V.I. Zakharov, Nucl. Phys. B **229**, 381 (1983).
20. M. Bianchi, S. Kovacs, G.C. Rossi, Lect. Notes Phys. **737**, 303 (2008) arXiv:hep-th/0703142.
21. M. Creutz, Ann. Phys. **326**, 911 (2011) arXiv:1007.5502 [hep-lat].
22. C. Bonati, M. D'Elia, Phys. Rev. D **89**, 105005 (2014) arXiv:1401.2441 [hep-lat].
23. UKQCD Collaboration (D.A. Smith *et al.*), Phys. Rev. D **58**, 014505 (1998) arXiv:hep-lat/9801008.
24. L. Del Debbio, H. Panagopoulos, E. Vicari, JHEP **08**, 044 (2002) arXiv:hep-th/0204125.
25. G. Bergner, P. Giudice, I. Montvay, G. Münster, U.D. Özugurel, S. Piemonte, D. Sandbrink, PoS **LATTICE2014**, 273 (2014) arXiv:1411.1746 [hep-lat].
26. M. Lüscher, S. Schaefer, JHEP **07**, 036 (2011) arXiv:1105.4749 [hep-lat].
27. M. Lüscher, S. Schaefer, JHEP **04**, 104 (2011) arXiv:1103.1810 [hep-lat].
28. R. Sommer, PoS **LATTICE2013**, 015 (2014) arXiv:1401.3270 [hep-lat].